Supporting Information

Beyond cadmium yellow: CdS photonic crystal pigments with vivid structural colors

Wuke Wei[#a], Chengcai Wu[#a], Qianyao Fang[a], Zhongwen Zhao[a] and Xin Su[*a]

School of Material Science and Chemical Engineering, Ningbo University, Ningbo, Zhejiang, 315211, China.

Table S1. Recipes for preparing monodisperse CdS spheres with various diameters

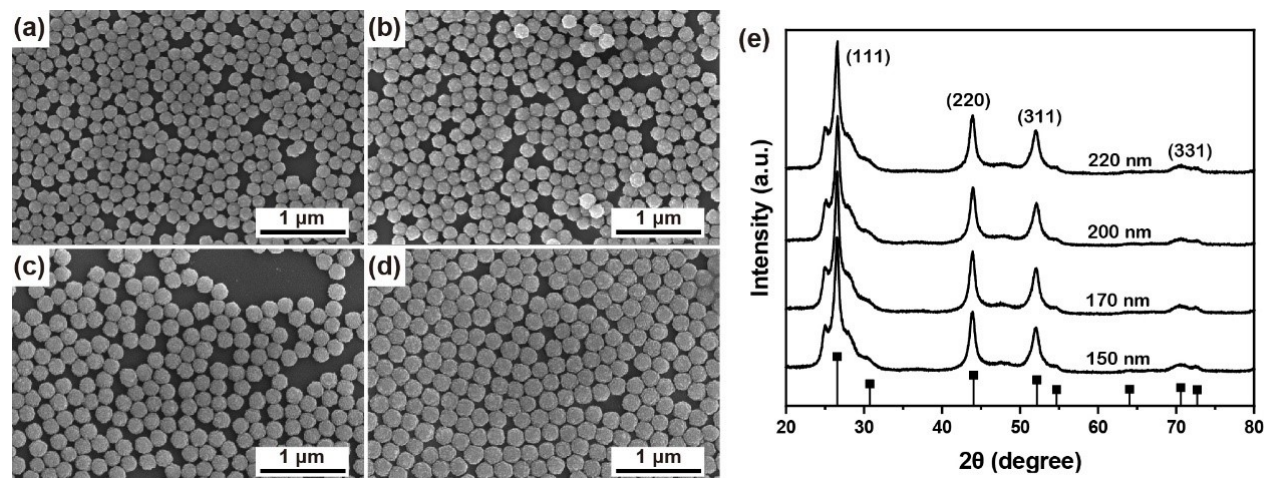| Cd(NO$_3$)$_2$·4H$_2$O (g)	TU (g)	PVP (g)	DEG (mL)	Diameter (nm)
11.72	2.89	5	360	150
12.34	3.04	5	360	170
12.96	3.20	5	360	200
13.57	3.35	5	360	220

Figure S1. SEM images of monodisperse CdS spheres with different diameters: (a) 150 nm; (b) 170 nm; (c) 200 nm; (d) 220 nm; (e) XRD patterns of CdS spheres

Table S2. Relations of shell thickness versus reaction time

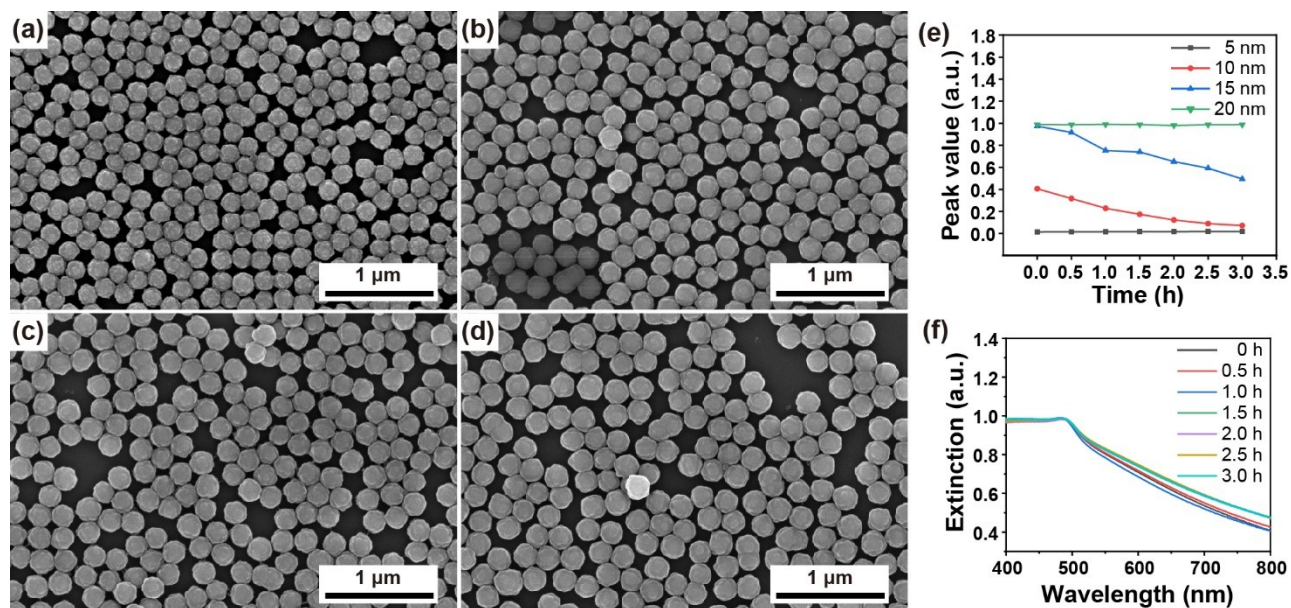| Reaction time (min)	thickness (nm)
30	5
60	10
90	15
120	20

Figure S2. SEM images of monodisperse CdS@SiO$_2$ core-shell spheres with 220 nm CdS as cores and various SiO$_2$ shell thickness: (a) 5 nm; (b) 10 nm; (c) 15 nm; (d) 20 nm; (e) peak intensity of extinction spectra of CdS@SiO$_2$ spheres at 480 nm with various shell thickness dispersed into HCl solution for different durations; (f) extinction spectra of 260 nm CdS@SiO$_2$ spheres (20 nm shell thickness) dispersed in HCl solution for different durations
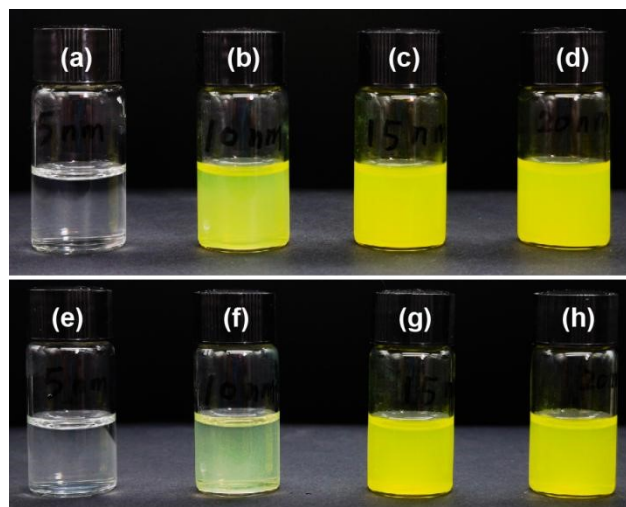
Figure S3. Digital photographs of CdS@SiO$_2$ spheres with various shell thickness dispersed in HCl solution for different durations: (a,e) 5 nm; (b,f) 10 nm; (c,g) 15 nm; (d,h) 20 nm; (a~d) 0 h; (e~h) 3h

Table S3. Zeta potential of CdS and CdS@SiO$_2$ spheres with various diameters

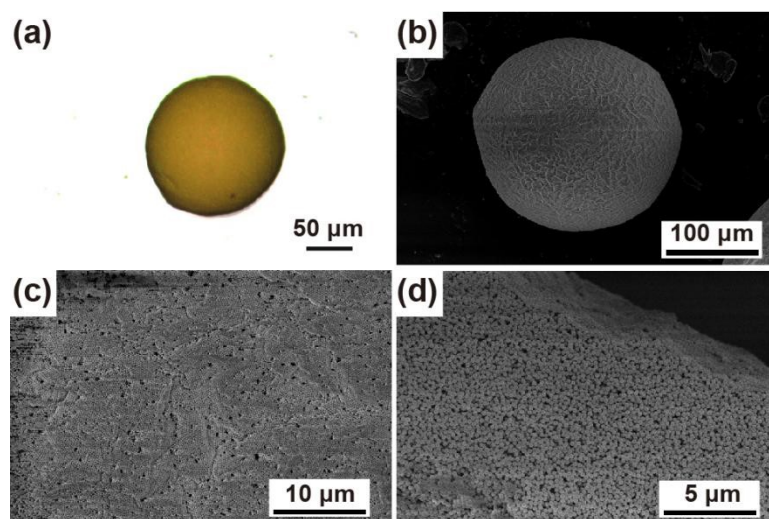| Spheres	Diameter (nm)	Zeta potential (mV)
CdS	170	-29.6
	200	-30.7
	220	-29.6
CdS@SiO$_2$	210	-45.7
	240	-44.8
	260	-44.9

Figure S4. (a) Optical image of a CdS PC ball; (b~d) SEM images of a CdS PC ball with different magnification times
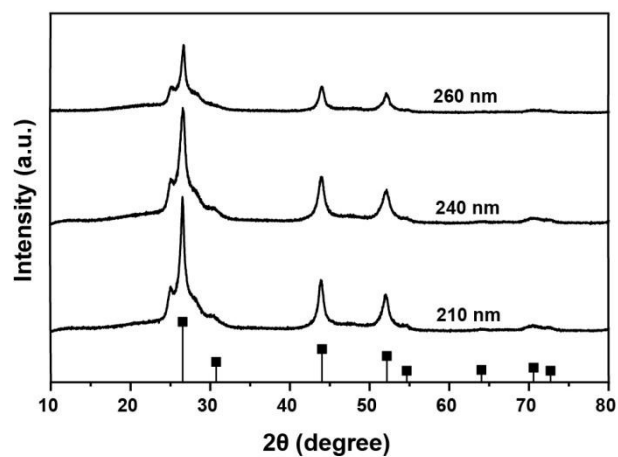

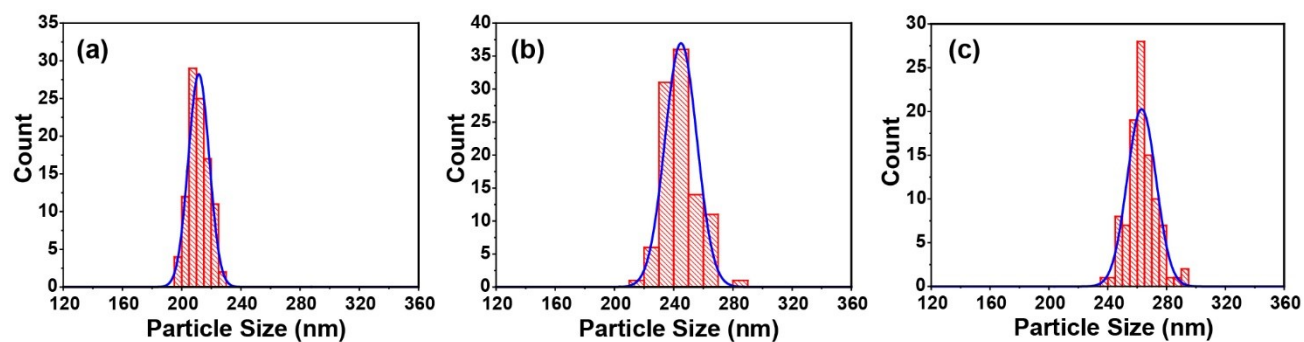**Figure S5.** XRD patterns of CdS@SiO$_2$ spheres with different diameters and identical 20 nm SiO$_2$ shells

Figure S6. Size distribution of CdS@SiO$_2$ core-shell spheres with various diameters: (a) 210 nm; (b) 240 nm; (c) 260 nm

Table S4. Theoretical and measured reflection peaks of CdS@SiO$_2$ PC balls

D$_{core}$ (nm)	D$_{core-shell}$ (nm)	Theoretical peaks (nm)	Measures peaks (nm)
170	210	639	524
200	240	746	578
220	260	817	680

The theoretical reflection peak positions can be calculated based on Bragg diffraction equation (1).

$$\lambda = 2d \sqrt{n_{eff}^2 - sin^2\theta} \qquad (1)$$

$$d = \sqrt{\frac{2}{3}} D \qquad (2)$$

$$n_{eff}^2 = f_{sphere} n_{sphere}^2 + f_{air} n_{air}^2 \qquad (3)$$

In these three equations, d is the distance between two neighboring crystalline planes in the (111) direction for a face-centered cubic (fcc) close-packed structure, and its relation with the sphere diameter D is shown in eqn (2). The effective refractive index (n_{eff}) can be approximated according to eqn (3). The incident angle θ is 0° for all samples. n_{sphere} and n_{air} stand for the refractive index of building blocks and air (n=1.00). In a fcc structure, the fill ratios of spheres (f_{sphere}) and air (f_{air}) are 0.74 and 0.26, respectively. Herein, as the building blocks are actually core-shell composite spheres, their effective refractive index can be approximated by the following equation (4). The refractive index of CdS cores and SiO$_2$ shells are 2.51 and 1.46, respectively. Based on the above data, the theoretical reflection peak positions can be calculated and summarized in Table S4."

$$n_{sphere}^2 = \frac{R_{core}^3}{R_{core-shell}^3} * n_{core}^2 + (1 - \frac{R_{core}^3}{R_{core-shell}^3}) * n_{shell}^2 \qquad (4)$$
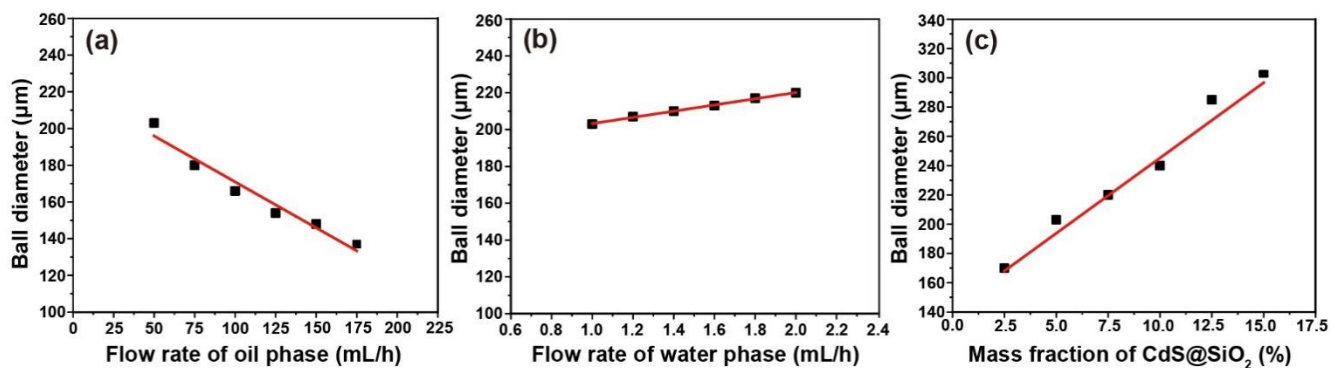
Figure S7. (a) The plot of PC ball diameter as a function of flow rate of oil phase; The flow rate and mass fraction of water phase is 1 mL/h and 5%, respectively. (b) the plot of PC ball diameter as a function of flow rate of water phase; The flow rate of oil phase and mass fraction of water phase is 50 mL/h and 5%, respectively. (c) the plot of PC ball diameter as a function of mass fraction of CdS@SiO$_2$ spheres in water phase; The flow rate of oil phase and water phase is 50 mL/h and 1 mL/h, respectively.
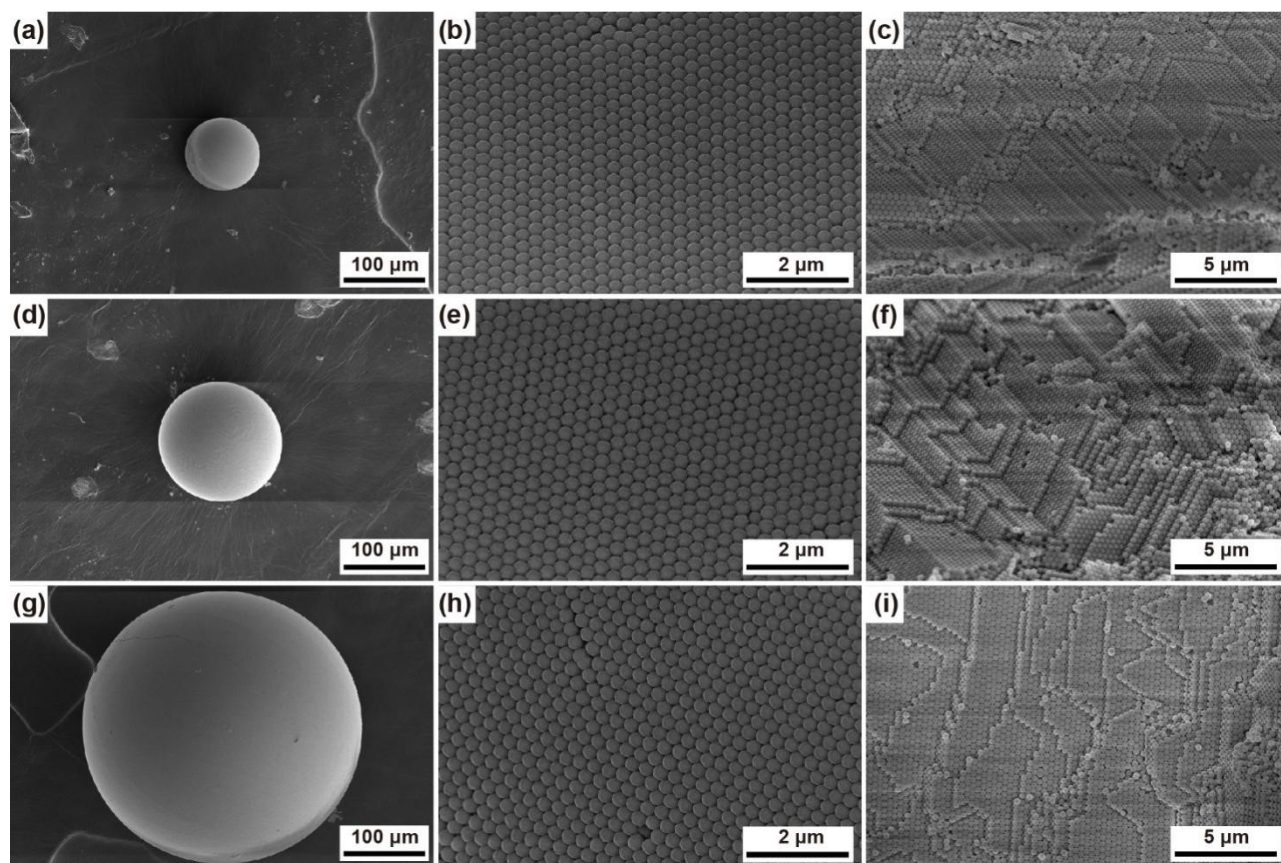
Figure S8. SEM images of PC balls with various sizes using 260 nm CdS@SiO$_2$ spheres as building blocks: (a-c) 80 μm; (d-f) 150 μm; (g-i) 340 μm
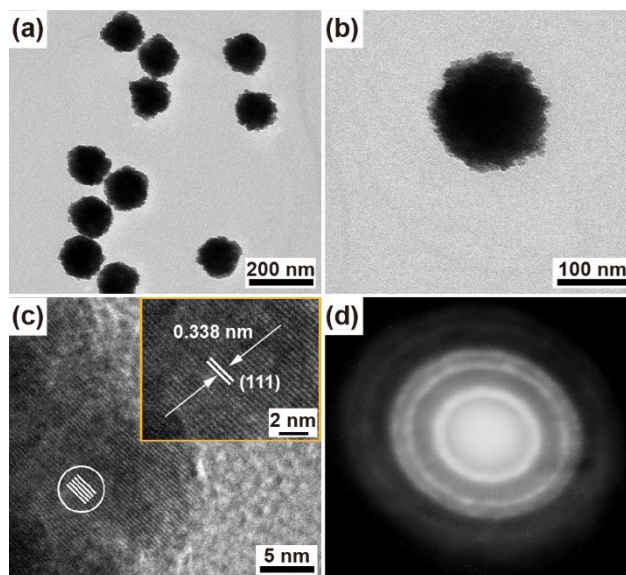
6

Figure S9. (a,b) TEM images of CdS spheres; (c) HR-TEM image of a CdS sphere showing the nanocrystalline domain with PVP capped onto the surface of a nanocrystal; (d) selected area electron diffraction image of a CdS sphere showing the polycrystalline nature
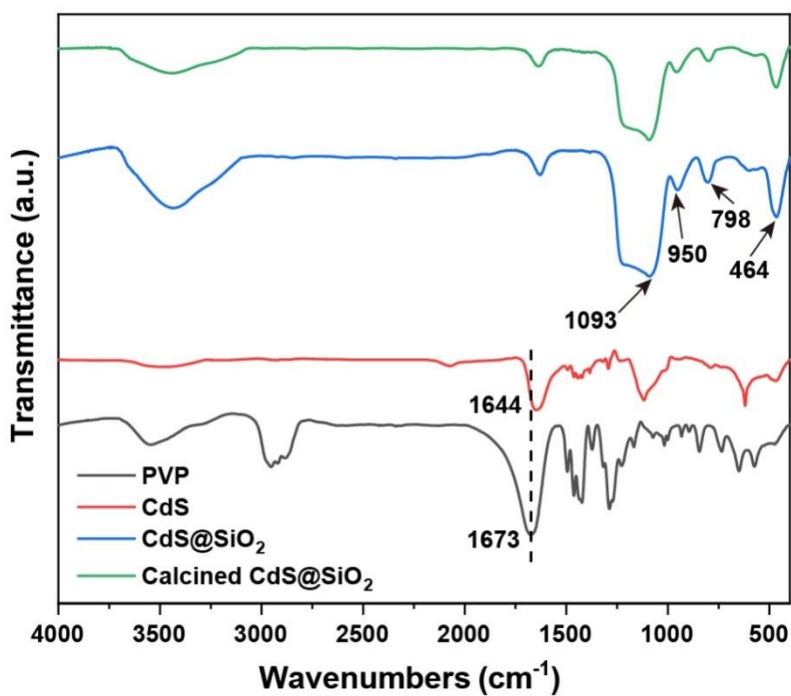

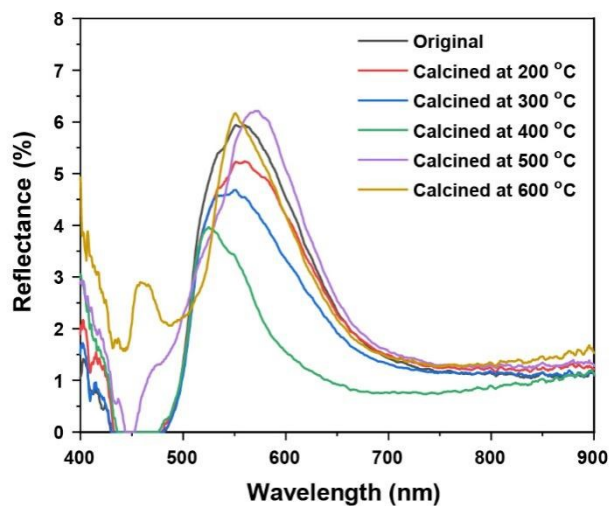**Figure S10.** FTIR spectra of PVP, CdS spheres, CdS@SiO$_2$ spheres before and after calcination

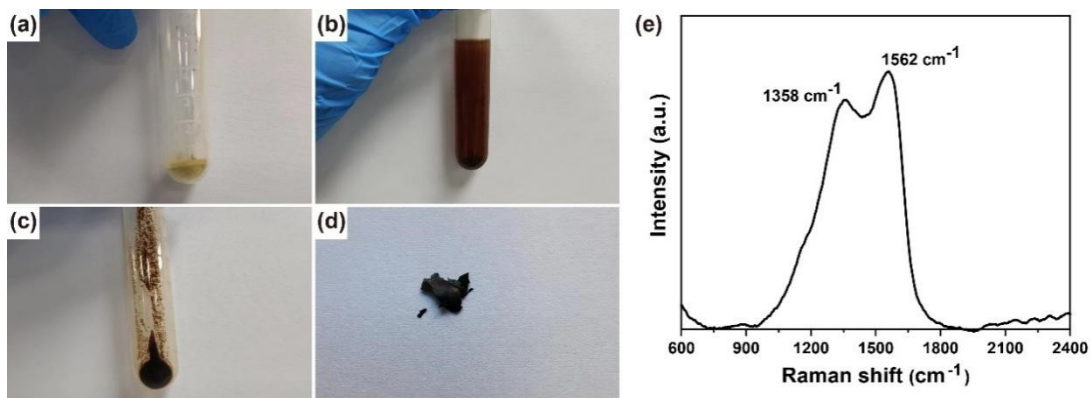**Figure S11.** Reflection spectra of CdS@SiO$_2$ PC balls annealed at various temperatures

Figure S12. Digital photographs of (a) CdS@SiO$_2$ spheres annealed at 400 °C for 2 h; (b) annealed CdS@SiO$_2$ spheres dispersed into the mixtures of concentrated hydrochloric acid and HF acid; (c) harvested etched products; (d) dried etched products; (e) Raman spectrum of d
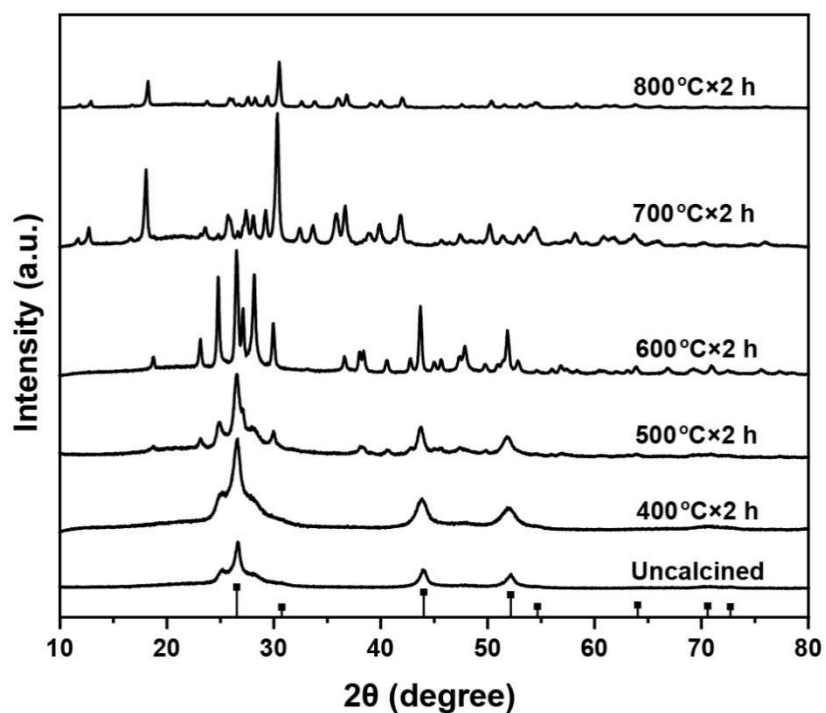
Figure S13. XRD patterns of CdS@SiO$_2$ PC balls calcined at different temperatures for 2 h
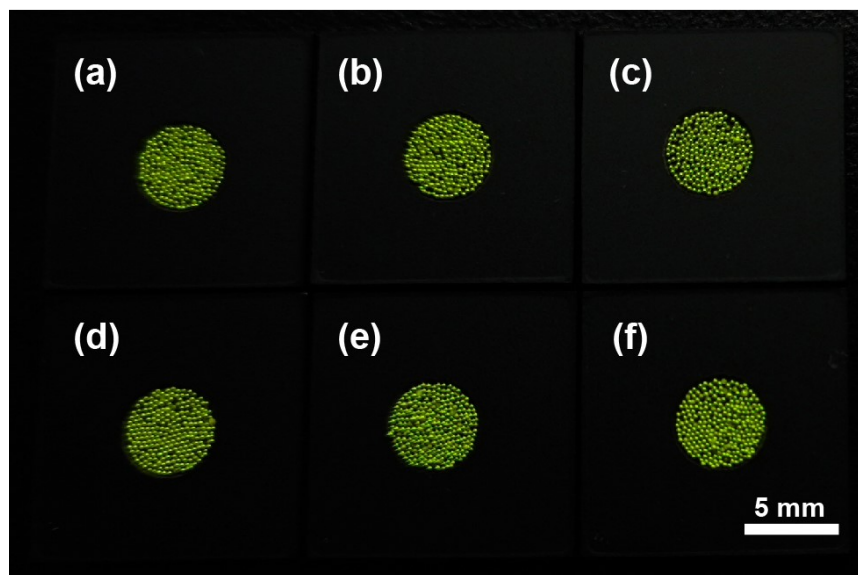

Figure S14. Digital photographs of PC pigments with 210 nm CdS@SiO$_2$ spheres as building blocks calcined at 400 °C for various durations: (a) 0.5 h; (b) 1 h; (c) 2 h; (d) 4 h; (e) 6 h; (f) 8 h
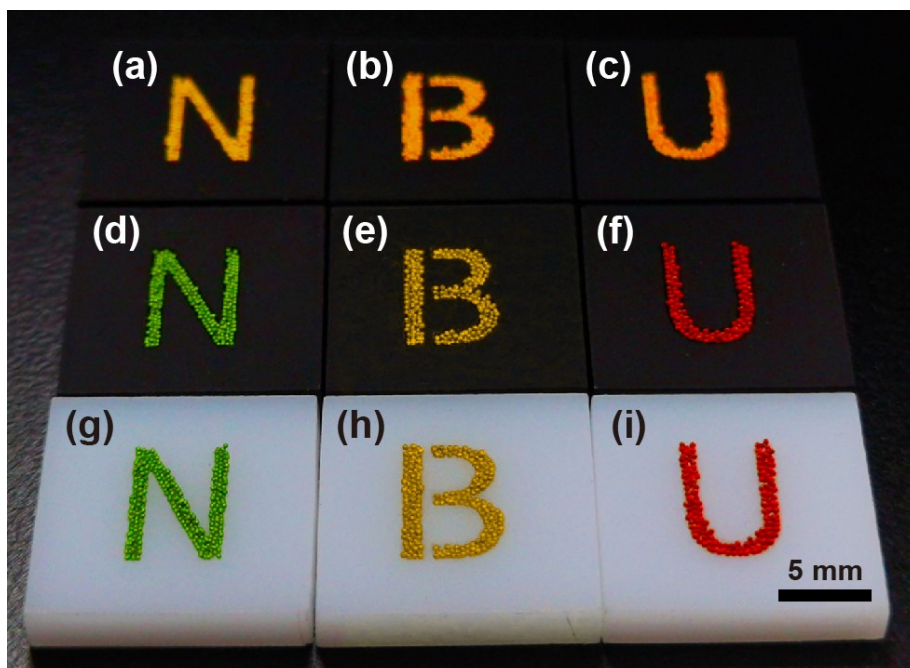
Figure S15. Digital photographs of CdS@SiO₂ PC balls and PC pigments shown in Figure 5 taken at a tilted observation direction, indicating angle-independent structural colors of CdS@SiO₂ PC pigments
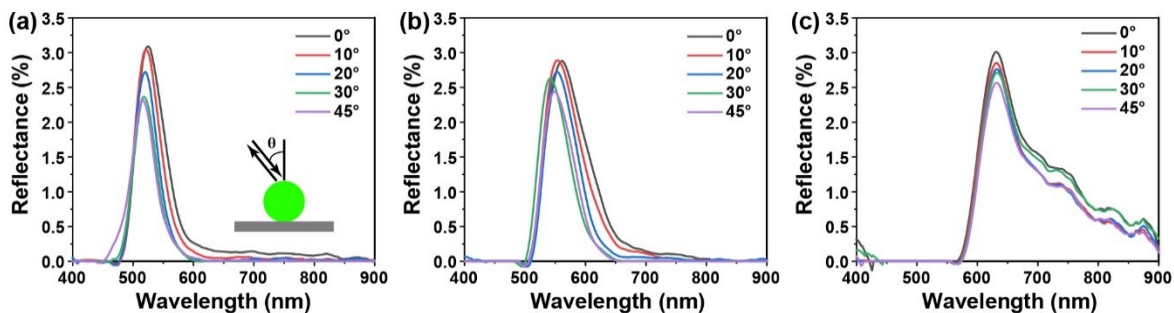

Figure S16. Angle-dependent reflection spectra of CdS@SiO₂ PC pigments: (a) green pigments; (b) yellow pigments; (c) red pigments
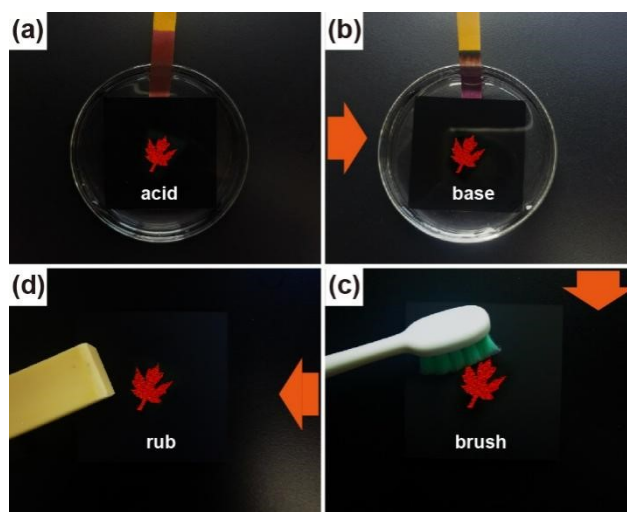
Figure S17. Digital photographs of a red leaf painting (a,b) soaked in acid solution (pH=2) and basic solution (pH=12) for 2 h; (c) brushed and (d) rubbed for 100 times